

HCOA*: Hierarchical Class-ordered A* for Navigation in Semantic Environments

Evangelos Psomiadis and Panagiotis Tsiotras

Abstract—This paper addresses the problem of robot navigation in mixed geometric and semantic 3D environments. Given a hierarchical representation of the environment, the objective is to navigate from a start position to a goal while minimizing the computational cost. We introduce Hierarchical Class-ordered A* (HCOA*), an algorithm that leverages the environmental hierarchy for efficient path-planning in semantic graphs, significantly reducing computational effort. We use a total order over the semantic classes and prove theoretical performance guarantees for the algorithm. We propose two approaches for higher-layer node classification based on the node semantics of the lowest layer: a Graph Neural Network-based method and a Majority-Class method. We evaluate our approach through simulations on a 3D Scene Graph (3DSG), comparing it to the state-of-the-art and assessing its performance against our classification approaches. Results show that HCOA* can find the optimal path while reducing the number of expanded nodes by 25% and achieving a 16% reduction in computational time on the uHumans2 3DSG dataset.

I. INTRODUCTION

As robotic sensing technologies advance, enabling robots to perceive vast and diverse information, two fundamental questions arise: *What information from this extensive data stream is most important for a given task, and how can the robot effectively utilize this information for decision-making?* Hierarchical semantic environment representations, such as 3D Scene Graphs (3DSG) [1]–[3], provide rich and structured abstractions that mirror human way of thinking, facilitating the selection and organization of information.

Previous research in hierarchical path-planning has primarily addressed the first question [4]–[7]. In [4] the authors introduce Hierarchical Path-Finding A*, a hierarchical A* variant for grid-based maps. Their approach partitions the map into clusters with designated entrance points, which are used for high-level path-planning. The authors in [5] propose a hierarchical graph search algorithm for graphs with edge weights represented as intervals. Similarly, in [7] the authors propose two hierarchical path-planning methods: path-making and alternating search direction.

Semantic path-planning has focused on the second question by incorporating semantics into the decision-making process. In [8] the authors introduce a weighted function that combines the edge cost and the semantic class to determine the optimal path, while considering the total order of the semantic classes. However, computing this weighted

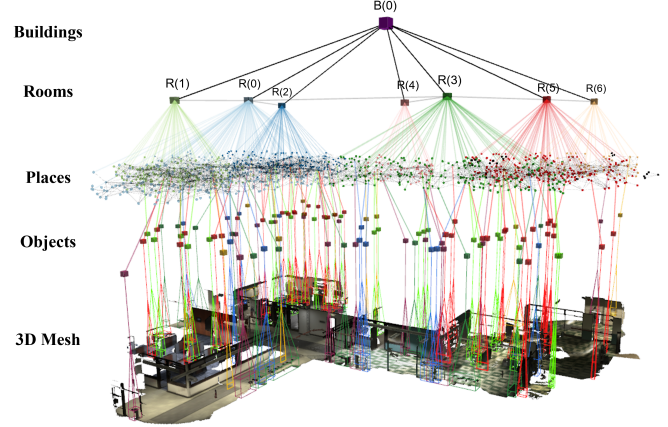


Fig. 1: 3D Scene Graph generated from the uHumans2 office scene dataset [16] using Hydra [2]. The graph comprises five layers, as shown in the figure. Room nodes are denoted as $R(\cdot)$, while building nodes are represented as $B(\cdot)$.

function requires global graph properties, which can be computationally demanding. To address this limitation, [9] and [10] propose Class-ordered A*/LPA*, two extensions of traditional A* [11] that efficiently incorporate semantics, based on a total order over the available classes. Building on the approaches of [5] and [9], in this paper, we develop a hierarchical class-ordered path-planning algorithm, enhancing scalability to larger and more complex environments.

Navigation within hierarchical semantic environments has also been explored in prior work. In [12], the authors introduce D-Lite, a set of two greedy, navigation-oriented compression algorithms for 3DSGs. These algorithms compress the graph based on the shortest path in the lowest layer, and the compressed representation is used for robot navigation. In [13], the authors address Task and Motion Planning in 3DSGs using a three-level hierarchical planner consisting of a discrete task planner, a navigation planner for path-planning, and a low-level planner. Their approach focuses on optimizing task planning to reduce computational cost, while path-planning operates on the unpruned 3DSG.

Learning-based methods have also been explored to facilitate task execution in a 3DSG. In [14], the authors propose HMS, a neural network-based approach for object search in a 3DSG, leveraging the 3DSG's hierarchy. In [15] and [3], the authors propose the Neural Tree, a Graph Neural Network (GNN) architecture designed for node classification. Although effective in classifying higher-layer nodes in 3DSGs, this approach requires a tree decomposition of the input graph, which increases computational time.

The work was supported by ARL award DCIST CRA W911NF-17-2-0181 and ONR award N00014-23-1-2304.

E. Psomiadis, and P. Tsiotras are with the D. Guggenheim School of Aerospace Engineering, Georgia Institute of Technology, Atlanta, GA, 30332-0150, USA. Email: {epsomiadis3, tsiotras}@gatech.edu

Main Contributions: Our approach integrates task semantics directly into the path-planning process within a unified algorithm. By leveraging the hierarchical structure of the environment, we significantly reduce computational resource demands while ensuring efficient navigation. Our key contributions are as follows:

- 1) We introduce Hierarchical Class-ordered A*, a novel hierarchical semantic path-planning algorithm for navigation in hierarchical semantic environments.
- 2) We propose two methods for node classification on the higher layers of the hierarchy based on underlying semantic classes: a GNN-based method and a majority-class method.
- 3) We validate our approach on a publicly available 3DSG dataset, demonstrating its effectiveness in real-world scenarios.

II. PRELIMINARIES

We model the environment as a hierarchical semantic graph (HSG). Specifically, let $G = (V, E, \mathcal{K})$ be a graph with n layers, where V is the set of nodes, $E \subseteq V \times V$ is the set of edges, and $\mathcal{K} = 1, \dots, K$ represents a set of semantic classes ordered by decreasing priority. We denote the set of layers as L , where $\ell = 0$ is the lowest layer and $\ell = n$ is the highest layer (root). Each layer ℓ forms a connected weighted subgraph $G^\ell = (V^\ell, E^\ell, \mathcal{K})$, with an associated weight function $w : E^\ell \rightarrow \mathbb{R}^+$. We assume that each node in layer $\ell - 1$, for $\ell = 1, \dots, n$, is connected to exactly one node in layer ℓ , which we refer to as its parent node. More generally, we define an ancestor as a node's parent or any higher-layer predecessor in the hierarchy. We define the projection function $p : V \times L \rightarrow V$ that maps each node to its corresponding ancestor in layer ℓ . An example of an HSG is the 3D Scene Graph (3DSG) shown in Figure 1.

Each node in $\ell = 0$ is assigned a semantic class based on perception data using the function $\phi_V^0 : V^0 \rightarrow \mathcal{K}$. We extend the labeling function ϕ_V^0 to layers $\ell \neq 0$. Details on the computation of ϕ_V^ℓ for $\ell \neq 0$ will be given in Section V. Additionally, we introduce the function $\phi_E^\ell : E^\ell \rightarrow \mathcal{K}$, which assigns semantic classes to the edges of G . Specifically, we define the edge classification function for an edge $e = (v, u)$ as $\phi_E^\ell(e) = \max(\phi_V^\ell(v), \phi_V^\ell(u))$, thereby overestimating the edge class.

Let $\Pi(v_s^\ell, v_g^\ell)$ denote the set of all acyclic paths in G^ℓ from $v_s^\ell \in V^\ell$ to $v_g^\ell \in V^\ell$, and let Π_k be the subset of Π in which the least favorable (i.e., highest) edge class is exactly k . Formally,

$$\Pi_k = \{\pi : N(\pi, k) > 0 \text{ and } N(\pi, k') = 0, \forall k' > k\}, \quad (1)$$

where $N(\pi, k) = |\{e \in \pi : \phi_E^\ell(e) = k\}|$ is the number of edges of class k in path π . We further define $\Pi_k^i \subseteq \Pi_k$ consisting of paths that contain exactly i edges of class k , that is $\Pi_k^i = \{\pi \in \Pi_k : N(\pi, k) = i\}$. To enable a consistent comparison of paths across different classes, we impose a total order such that $k < \ell \Rightarrow \Pi_k^i \prec \Pi_\ell^j$ for all i, j and $i < j \Rightarrow \Pi_k^i \prec \Pi_k^j$. This order ensures that any two paths with the same start and goal nodes can be compared.

Algorithm 1 Hierarchical Class-ordered A* (HCOA*)

Input: $G, v_s, v_g, h(v)$

Output: π^0

```

1: for all  $\ell = \ell_n, \dots, \ell_0$  do
2:    $v_s^\ell \leftarrow p(v_s, \ell); v_g^\ell \leftarrow p(v_g, \ell)$ 
3:    $g(v_s^\ell) \leftarrow 0; \theta(v_s^\ell) \leftarrow 0 \cdot \mathbf{1}_K; f(v_s^\ell) \leftarrow h(v_s^\ell)$ 
4:    $g(v^\ell) \leftarrow \infty; \theta(v^\ell) \leftarrow \infty \cdot \mathbf{1}_K, \forall v^\ell \in G \setminus \{v_s^\ell\}$ 
5:   PredecessorMap  $\leftarrow \emptyset$   $\triangleright$  Track path reconstruction
6:    $Q \leftarrow \{v_s^\ell\}$   $\triangleright$  Initialize priority queue
7:   while  $Q$  is not empty do
8:      $v \leftarrow \text{POPNode}(Q); Q \leftarrow Q \setminus \{v\}$ 
9:     if  $v = v_g^\ell$  then
10:        $\pi^\ell \leftarrow \text{PATH}(\text{PredecessorMap}, v_g)$ 
11:       BREAK
12:     end if
13:     for all  $u \in \text{neighbors}(v, G^{\ell'})$  do
14:        $\theta(v, u) \leftarrow \text{SEMANTICS}(\phi_V^\ell(v), G^{0'}(u))$ 
15:       if  $(\theta(v) + \theta(v, u) \prec \theta(u))$  or
16:          $(\theta(v) + \theta(v, u) = \theta(u) \text{ and } g(v) + w(v, u) < w(u))$  then
17:          $Q \leftarrow Q \cup \{u\}$ 
18:         PredecessorMap[ $u$ ]  $\leftarrow v$ 
19:          $\theta(u) \leftarrow \theta(v) + \theta(v, u)$ 
20:          $g(u) \leftarrow g(v) + w(v, u)$ 
21:          $f(u) \leftarrow g(u) + h(u)$ 
22:       end if
23:     end for
24:   end while
25:   for all  $\ell' < \ell$  do
26:      $G^{\ell'} \leftarrow \{v \in G^{\ell'} : p(v, \ell) \in \pi^\ell\}$ 
27:   end for
28: end for
29: return  $\pi^0$ 

```

III. PROBLEM FORMULATION

Consider a mobile robot tasked with navigating a complex 3D environment where certain regions have lower traversal priority. The robot is provided with a HSG of the environment (e.g., 3DSG), as outlined in Section II, where the semantic classes of the nodes in layer $\ell = 0$ are assigned based on perception and tailored to the specific task (e.g. avoid certain objects). Let $v_s \in V^0$ and $v_g \in V^0$ denote the robot's starting and goal nodes, respectively. The objective is to determine the shortest path within layer $\ell = 0$ while minimizing traversal through the least favorable edges. Formally,

$$\pi^*(v_s, v_g) = \arg \min_{\pi \in \Pi^*(v_s, v_g)} \sum_{e \in \pi} w(e), \quad (2a)$$

$$\Pi^* = \min_{i \in \mathbb{N}} \min_{k \in \mathcal{K}} \Pi_k^i, \quad (2b)$$

where Π^* is the set of paths obtained by minimizing over all possible classes k and number of least favorable class i .

However, due to computational constraints, the robot seeks to avoid a full graph search over the entire G^0 , as its structure is both large and semantically diverse, potentially rendering the search intractable.

A. Problem Statement

We propose a hierarchical semantic path-planning algorithm for efficient robot navigation in large-scale environments. The algorithm operates top-down across the layers of the HSG, iteratively computing the optimal semantic path at each layer while pruning nodes that are not included in the selected path. Additionally, we introduce two methods for node classification to predict the semantic classes of higher-layer nodes: a Graph Neural Network (GNN)-based approach and a majority-class method.

IV. PATH-PLANNING

A. Hierarchical Class-ordered A*

We introduce Hierarchical Class-ordered A* (HCOA*), a hierarchical semantic path-planning algorithm for HSGs. The algorithm begins by finding a path in layer $\ell = n - 1$ and then refining it by recursively applying the same process at the lower levels of the hierarchy. By structuring the search hierarchically, the algorithm performs multiple searches on smaller subgraphs rather than executing a computationally expensive search over G^0 . At each layer, the algorithm utilizes Class-ordered A* (COA*) [9], which finds the shortest path while minimizing the number of least favorable edges through lexicographic comparison.

HCOA* is presented in Algorithm 1. We use the function $h : V \rightarrow \mathbb{R}$ to denote an admissible heuristic function, similar to standard A*. Lines 2–6 initialize the variables, where the function $p(v, \ell)$ returns the ancestor of node v in layer ℓ . Lines 7–24 execute COA*, which will be detailed in Section IV-B. Notably, Line 14 computes the semantic class of the edge (v, u) based on the semantic classes of nodes v and u . If $\ell = 0$, the nodes' semantics are determined from perception data, whereas for $\ell \neq 0$, they are predicted using the methods described in Section V. Additionally, $G^{0'}(u)$ is the induced subgraph of node u in layer $\ell = 0$ given by $G^{0'}(u) = \{u' \in V^0 : p(u', \ell) = u\}$. Finally, Lines 25–27 refine the path by pruning nodes that do not share an ancestor with the paths in the higher layers.

B. Class-ordered A*

In this section, we present an overview of the simplified COA* implementation used in HCOA* (Lines 7–24 in Algorithm 1) to help the reader understand the simplifications made on the baseline algorithm. Further details, along with proofs of the COA* optimality and completeness, can be found in [9].

Consider a single-layer, weighted, semantic graph G^ℓ . In this algorithm, each node v is characterized by the triple (q, g, θ) , where q is the predecessor node, $g : V^\ell \rightarrow \mathbb{R}^+$ is the cost-to-come function, and $\theta_V : V \rightarrow \mathbb{N}^K$ specifies the number of edges of each semantic class along the path up to node v . We extend θ_V to single edges by defining $\theta_E : E^\ell \rightarrow \mathbb{N}^K$ as an one-hot vector with all elements zero except at ϕ_E . The subscript is omitted in Algorithm 1. The function POPNODE selects the next node to expand lexicographically, and PATH constructs the optimal path by

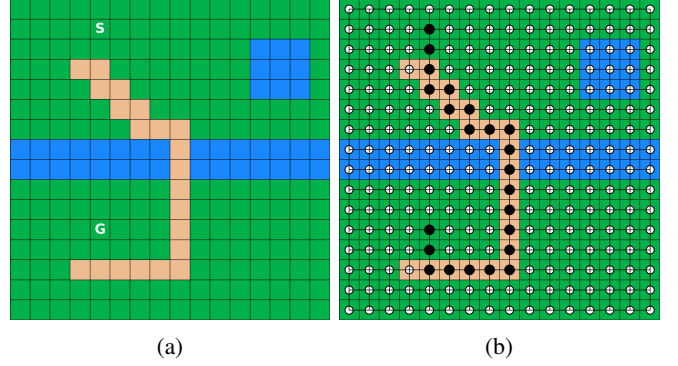


Fig. 2: (a) Grid environment with three semantic classes: road, grass, river. S denotes the starting cell while G denotes the target; (b) Associated graph of the environment and optimal path produced by Class-ordered A*.

backtracking through parent nodes from the goal. Figure 2 presents the path of COA* in a grid world environment.

C. Performance Guarantees

The following propositions establish the algorithm's completeness along with sufficient conditions for its optimality. For both propositions, we assume that the assumptions for completeness and optimality of COA* hold [9]. Proposition 2 relies on two key assumptions. While these assumptions may seem restrictive, they often hold in indoor environments, as discussed in Section VI.

Proposition 1: Let G be an HSG and let nodes $v_s, v_g \in V^0$. HCOA* is *complete*, meaning that it is guaranteed to find a path $\pi^0 = \pi(v_s, v_g)$, whenever one exists.

Proof: Let π^0 exists. The structure of G ensures that for each layer $\ell \in L$, there exists a corresponding path $\pi^\ell = \pi(v_s^\ell, v_g^\ell)$, where $v_s^\ell = p(v_s, \ell)$ and $v_g^\ell = p(v_g, \ell)$.

At each subgraph G^ℓ , COA* is guaranteed to find the optimal path $\pi^{\ell*}$, if one exists [9]. Suppose, ad absurdum, that the graph pruning performed in Lines 25–27 results in $\Pi(v_s^{\ell-1}, v_g^{\ell-1}) = \emptyset$, preventing COA* from finding a solution in layer $\ell - 1$. This would imply that $\pi^{\ell*}$ is disconnected, contradicting the completeness of COA*. ■

Proposition 2: Let G be an HSG with nodes $v_s, v_g \in V^0$. Suppose that in layer $\ell = 1$, the acyclic path $\pi^1(v_s^1, v_g^1)$ is unique, and that for all $u_s, u_g \in V^0$ sharing the same parent, $P = p(u_s, 1) = p(u_g, 1)$, every node u along the optimal path $\pi^*(u_s, u_g)$ satisfies $p(u, 1) = P$. Then, HCOA* is guaranteed to find the optimal path $\pi^*(v_s, v_g)$.

Proof: Define $G^{0'} \subseteq G^0$ as the pruned graph after n iterations of HCOA*. Suppose, ad absurdum, that a segment of the optimal path $\pi^*(v_s, v_g)$ was removed, i.e., there exists a sub-path $\hat{\pi} \subseteq \pi^*(v_s, v_g)$ such that $\hat{\pi} \not\subseteq G^{0'}$. Two cases arise: (i) The parents of $\hat{\pi}$ in layer $\ell = 1$ form a cycle that starts and ends at a parent of a node in $\pi^*(v_s, v_g) \cap G^{0'}$. This contradicts the second assumption, which states that the nodes of the optimal path at $\ell = 0$ where the starting and goal node share the same parent, must all have the same parent. (ii) The parents of $\hat{\pi}$ in layer $\ell = 1$ are part of a sub-path that starts at the parent of one node in $\pi^*(v_s, v_g) \cap G^{0'}$ and ends

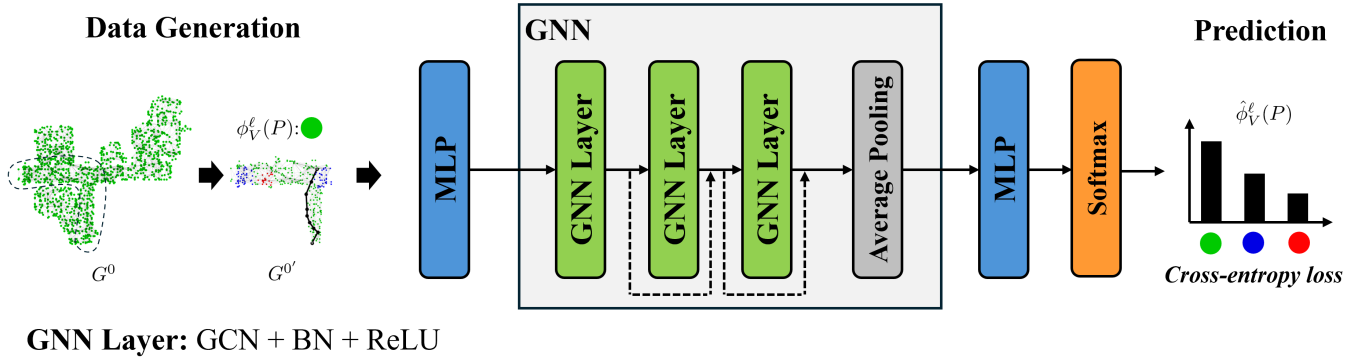


Fig. 3: Proposed GNN architecture for node $P \in V^\ell$ ($\ell \neq 0$) classification, utilizing the semantic classes (green, blue, red) of nodes in $\ell = 0$. The dataset $\mathcal{D} = \{G^{0'}(P), \phi_V^\ell(P)\}$ is generated by running COA* on subgraphs of induced nodes. The network consists of two MLPs for pre-processing and post-processing, three GNN layers with skip connections, and an average pooling operator. Training is conducted using cross-entropy loss over the semantic classes.

at a different parent of another node in $\pi^*(v_s, v_g) \cap G^{0'}$. This contradicts the first assumption, as it implies the existence of two distinct paths in layer $\ell = 1$, violating uniqueness. ■

V. SEMANTIC CLASS PREDICTION

Let $\phi_V^\ell : V^\ell \rightarrow \mathcal{K}$ be the function that assigns semantic classes to nodes in the layers $\ell \neq 0$. Ideally, given an optimal path $\pi^*(v_s, v_g)$ computed in G^0 , the semantic class of a node $P \in V^\ell$ is determined conservatively by selecting the highest semantic class present in the nodes in $\ell = 0$ that both belong to the optimal path and are part of the subgraph $G^{0'}(P) = \{u \in V^0 : p(u, \ell) = P\}$ induced by P in layer $\ell = 0$. Formally, this is expressed as:

$$\phi_V^\ell(P) = \max_{u \in \pi^*(P)} \phi_V^0(u), \quad (3a)$$

$$\pi^*(P) = \pi^*(v_s, v_g) \cap G^{0'}. \quad (3b)$$

This process follows a bottom-up approach, necessitating the computation of the optimal path in layer $\ell = 0$. Given that HCOA* works top-down, we seek an alternative method to assign semantic classes to the higher layers. In the next sections, we present the proposed approaches to predict the semantic classes of higher-layer nodes.

A. Graph Neural Network Method

We formulate this problem as a supervised node classification task and design a GNN to predict the semantic classes. We construct a dataset $\mathcal{D} = \{G^{0'}(P), \phi_V^\ell(P)\}$ by selecting nodes $P \in V^\ell$ for $\ell \neq 0$ and extracting their induced subgraphs $G^{0'}(P)$. We then assign semantic classes to the nodes in $G^{0'}(P)$ based on the given task. For instance, if the task is navigation with object avoidance, we can assign different priorities to regions by placing disks of a specified radius and semantic class around certain object nodes. Next, we execute COA* on this graph and compute $\phi_V^\ell(P)$, where the starting location is a border node.

A border node $v^* \in V^0$ of layer ℓ is defined as a node that shares an edge with another node from a different ancestor. Formally, there exists $e = (v^*, u^*)$ where $v^*, u^* \in V^0$ and $p(v^*, \ell) \neq p(u^*, \ell)$. Border nodes play a crucial role in the

classification of $P \in V^\ell$. If the start and goal nodes do not share the same ancestor, the optimal path must traverse a border node in layer ℓ . Conversely, if both nodes have P as their ancestor, the classification of P becomes irrelevant, as HCOA* will not need to compute a path in layer ℓ .

The proposed model is illustrated in Figure 3. We use border nodes as input features for the network, which are concatenated with the semantic classes of the nodes in $G^{0'}$ represented as one-hot encodings. A 2-layer MLP is used to preprocess the input.

The GNN consists of three layers, each incorporating a Graph Convolutional Network (GCN) operator [17] for message passing, followed by batch normalization and a ReLU activation. To mitigate oversmoothing, we introduce skip connections between the GNN layers. Additionally, we apply average pooling to handle environments of varying sizes. The pooled representation is then processed through another 2-layer MLP, followed by a softmax function. Finally, we use cross-entropy as the loss function for node classification. Formally, given a dataset \mathcal{D} and learnable parameters $\vartheta_{\text{GNN}}, \vartheta_{\text{MLP}}$, the predicted semantic class is obtained by:

$$\min_{\vartheta_{\text{GNN}}, \vartheta_{\text{MLP}}} \sum_{(G^{0'}(P), \phi_V^\ell(P)) \in \mathcal{D}} \mathcal{L}_{\text{CE}}(\hat{\phi}_V^\ell(P), \phi_V^\ell(P)), \quad (4)$$

where $\hat{\phi}_V^\ell = f(G^{0'}(P); \vartheta_{\text{GNN}}, \vartheta_{\text{MLP}})$ represents the model function parametrized by $\vartheta_{\text{GNN}}, \vartheta_{\text{MLP}}$.

B. Majority-Class Method

The Majority-Class (MC) method is a simple and fast approach for predicting the semantic class of a node $P \in V^\ell$ for $\ell \neq 0$ by directly calculating the semantic classes of the nodes in $G^{0'}(P)$. Specifically, the predicted class is determined by counting the occurrences of each semantic class among the nodes in the induced subgraph $G^{0'}(P)$ and selecting the most frequent one. That is,

$$\hat{\phi}_V^\ell(P) = \arg \max_{k \in \mathcal{K}} N_V(G^{0'}(P), k), \quad (5)$$

where $N_V(G, k) = |\{v \in G : \phi_V^0(v) = k\}|$ is the number of nodes of class k in G .

TABLE I: Room Node Classification.

Metrics	GNN	MC
Training Time (min)	90	-
Validation Accuracy (%)	67.64	30.36
Test Accuracy (Rooms with 1-20 bn) (%)	82.50	54.25
Test Accuracy (Rooms with 21-30 bn) (%)	65.00	19.75
Test Accuracy (Rooms with 31-40 bn) (%)	64.00	19.25
Test Accuracy (Rooms with 41-50 bn) (%)	59.00	24.50

VI. SIMULATIONS

We perform two sets of simulations on the publicly available uHumans2 office 3DSG, shown in Figure 1 and constructed using Hydra [2]. In the figure, the corresponding layers are also depicted. The **places** layer $\ell = 0$ is a subgraph where each node represents an obstacle-free location, and edges indicate straight-line traversability. The rooms at layer $\ell = 1$ consist of nodes representing room centers, with edges connecting neighboring rooms. The number of border nodes (bn) and places in each room are:

R(0): 49 bn, 330 places, R(1): 22 bn, 259 places, R(2): 30 bn, 196 places, R(3): 32 bn, 195 places, R(4): 4 bn, 63 places, R(5): 35 bn, 206 places, R(6): 14 bn, 65 places.

We consider a set of three semantic classes \mathcal{K} , ordered by decreasing priority: 1 (Green), 2 (Blue), 3 (Red). We utilize the **objects** layer to identify objects and assign semantic classes to the surrounding **place** nodes.

In the first section, we present the training results of the GNN and its comparison with the MC approach. The second section demonstrates a path-planning scenario on the entire 3DSG and compares HCOA*, using both the GNN and MC methods, against COA*. HCOA*-GNN utilizes the best GNN model from the previous training phase for room inference. All the simulations were performed using Python 3.8.10 and PyTorch 2.4.1 on a computer with 2.2 GHz, 12-Core, Intel Core i7-8750H CPU, 16GB RAM and an Nvidia RTX 2060 GPU, 6GB VRAM.

A. Performance Metrics

To evaluate the performance of room classification, we compute the accuracy, which measures the proportion of correctly classified rooms in each dataset:

$$\text{Accuracy} = \frac{\sum_{i=1}^n \mathbb{1}(\hat{\phi}_V^\ell(P_i) = \phi_V^\ell(P_i))}{n}, \quad (6)$$

where n is the number of samples, and $\mathbb{1}(\cdot)$ is the indicator function, which equals 1 if the predicted class matches the ground truth and 0 otherwise.

For the path-planning scenario in the whole 3DSG, we compute the computational time of the algorithms along with the number of expanded nodes (Line 8 in Algorithm 1).

B. Room Node Classification

In this section, we present the results from predicting the semantic class of room nodes. To generate the dataset, we constructed 14,000 graphs by extracting the induced subgraphs from all rooms and randomly assigning semantic classes to nodes within a disk of randomly chosen center

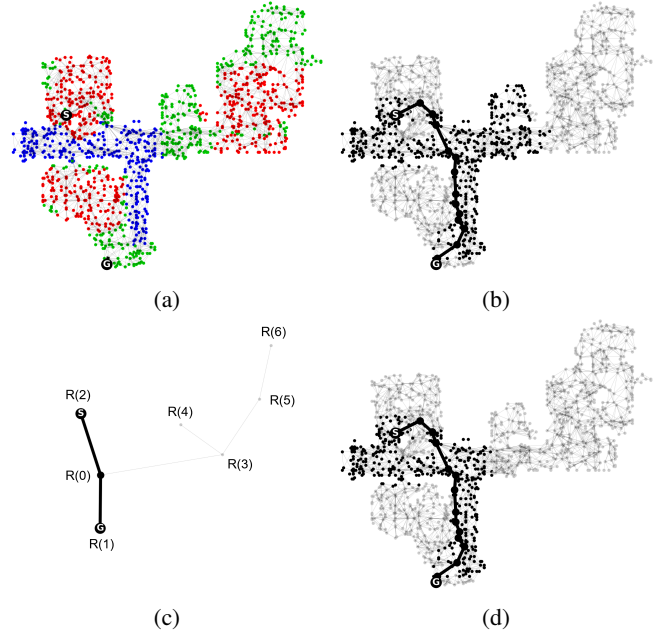


Fig. 4: (a) Places subgraph of the uHumans2 office scene (52m×45m) with the assigned semantic classes (green, blue, red). The starting node is denoted by **S**, and the goal node by **G**; (b-d) The path of each algorithm is shown in bold black. Expanded nodes are depicted in regular black, while unexpanded nodes in gray: (b) Path of COA* on the places subgraph; (c) Path of HCOA* on the rooms subgraph; (d) Path of HCOA* on the places subgraph.

locations, repeating this process 2,000 times per room. Then, we ran COA* to determine the semantic class of the room, starting from a randomly selected border node. The dataset was split into 80% training, 10% validation, and 10% testing. The model was trained using the Adam optimizer [18] with a learning rate of 10^{-2} , over 1,600 epochs, a dropout rate of 0.2 and a batch size of 64. The GNN and MLP layers contain 32 neurons.

Table I summarizes the results of room node classification. For the test set, we analyze performance separately for rooms with different numbers of border nodes. The results indicate that the GNN approach outperforms significantly the MC method across both the validation and test sets. Additionally, the training accuracy of the GNN is 67.94%.

C. Path-Planning on uHumans2 Office Scene

In this section, we demonstrate a path-planning scenario in the 3DSG shown in Figure 1. The starting node v_s is in R(2), while the goal v_g is in R(1). For the environment's semantic classes, we assign $\phi_V^0(v) = 2$, for all $v \in R(0)$ (e.g., R(0) represents a typically crowded area, which the robot should try to avoid). Additionally, we define $\phi_V^0(v) = 3$, for all $v \in C$, where C is the set of **place** nodes located within a disk centered around specific objects. Formally, $C = \{v \in G^0 : \|x(v) - x(o)\|_2 \leq r, \forall o \in O\}$, where $x(\cdot)$ denotes the location of a **place** node v or an object o , and O is a set of objects. In this scenario, we set $r = 3\text{m}$ and define O as the set of all computers in the 3DSG. This means that the

TABLE II: Path-Planning on uHumans2 Office Scene.

Metrics	HCOA*-GNN	HCOA*-MC	COA*
Expanded Nodes	412	412	549
Time (10^{-3} s)	38.8 ± 47.1	4.3 ± 2.6	5.1 ± 2.5
Optimal Path	✓	✓	✓

robot should avoid passing too close to computers for safety reasons, as they might be in use by humans. Figure 4(a) depicts the **places** layer of the environment along with the start and goal nodes.

The computed path of COA* in the **places** layer is shown in Figure 4(b). Figures 4(c)-(d) illustrate the results of HCOA* in the **rooms** and **places** layers, respectively. The figures also show the expanded nodes for each algorithm. In particular, COA* expanded nodes in two additional rooms compared to HCOA*. The exact number of expanded nodes is provided in Table II, where HCOA* demonstrates a 25% reduction in expanded nodes compared to COA*.

Table II also presents the computational time of the algorithms over 1,000 runs. We observe that HCOA*-MC achieves the best performance in terms of computational efficiency, reducing the execution time by 16% compared to COA*. However, HCOA*-GNN has the highest computational time, as GNN inference can be more time-consuming than graph search in small graphs (the entire **places** sub-graph contains only 1,314 nodes). It should be noted that the first run of HCOA*-GNN takes longer, likely due to compilation and GPU/CPU warm-up overhead. Additionally, both GNN and MC classify R(0) as class 2 and R(2) as class 3. However, while the GNN assigns class 3 to R(3), MC classifies it as class 1. The remaining rooms are not classified, as they are not adjacent to any expanded nodes.

Finally, all three approaches successfully compute the optimal path in the **places** layer, as shown in Figure 4. It is important to note that while the first assumption of Proposition 2 holds, the second assumption does not. However, this does not affect the results in this case, as the optimal path in the **places** layer does not require deviations into rooms outside the unique path in the **rooms** layer to achieve a lower-cost trajectory.

VII. CONCLUSIONS

In this paper, we addressed the problem of robot navigation in 3D geometric and semantic environments by leveraging the hierarchical structure of the environment for efficient path-planning. We introduced Hierarchical Class-ordered A* (HCOA*), an algorithm that exploits a total order over semantic classes to guide the search process while significantly reducing computational effort. To classify higher-layer nodes, we proposed two methods: a Graph Neural Network-based method and a Majority-Class method. Through simulations on a 3D Scene Graph, we showed that HCOA* effectively reduces computational cost compared to a state-of-the-art method. Specifically, our results show that HCOA* finds the optimal path while reducing the number of expanded nodes by 25% and achieving a 16% reduction in computational time for a typical 3DSG with 1,314 nodes.

Moving forward, future work will focus on applying HCOA* to larger, real-world datasets to demonstrate the full potential of the algorithm. Additionally, we aim to develop an online path-planning framework based on HCOA*, enabling adaptive decision-making in real-time, dynamic scenarios.

REFERENCES

- [1] I. Armeni, Z.-Y. He, J. Gwak, A. R. Zamir, M. Fischer, J. Malik, and S. Savarese, “3D Scene Graph: A structure for unified semantics, 3D space, and camera,” in *IEEE International Conference on Computer Vision (ICCV)*, Seoul, Korea, Oct 27 - Nov 02 2019, pp. 5663–5672.
- [2] N. Hughes, Y. Chang, and L. Carlone, “Hydra: A real-time spatial perception system for 3D scene graph construction and optimization,” in *Robotics: Science and Systems (RSS)*, New York, NY, June 27 – July 1 2022.
- [3] N. Hughes, Y. Chang, S. Hu, R. Talak, R. Abdulhai, J. Strader, and L. Carlone, “Foundations of spatial perception for robotics: Hierarchical representations and real-time systems,” *The International Journal of Robotics Research*, vol. 43, no. 10, pp. 1457–1505, Feb 2024.
- [4] A. Botea, M. Müller, and J. Schaeffer, “Near optimal hierarchical path-finding (HPA*),” *Journal of Game Development*, vol. 1, pp. 1–30, Jan 2004.
- [5] J. Fernandez and J. Gonzalez, “Hierarchical graph search for mobile robot path planning,” in *IEEE International Conference on Robotics and Automation (ICRA)*, vol. 1, Leuven, Belgium, May 16-21 1998, pp. 656–661.
- [6] C. W. Warren, “Fast path planning using modified A* method,” in *IEEE International Conference on Robotics and Automation (ICRA)*, vol. 2, Atlanta, GA, May 1993, pp. 662–667.
- [7] R. Holte, C. Drummond, M. Perez, R. Zimmer, and A. Macdonald, “Searching with abstractions: A unifying framework and new high-performance algorithm,” in *Canadian Conference on Artificial Intelligence*, Banff, Canada, Jan 1994, pp. 263–270.
- [8] D. Wooden and M. Egerstedt, “On finding globally optimal paths through weighted colored graphs,” in *IEEE Conference on Decision and Control (CDC)*, San Diego, CA, Dec 13-15 2006, pp. 1948–1953.
- [9] J. Lim and P. Tsotras, “A generalized A* algorithm for finding globally optimal paths in weighted colored graphs,” Dec 2020, arXiv:2012.13057.
- [10] J. Lim, O. Salzman, and P. Tsotras, “Class-ordered LPA*: An incremental-search algorithm for weighted colored graphs,” in *IEEE/RSJ International Conference on Intelligent Robots and Systems (IROS)*, Prague, Czech Republic, Sep 27 - Oct 01 2021, pp. 6907–6913.
- [11] P. E. Hart, N. J. Nilsson, and B. Raphael, “A formal basis for the heuristic determination of minimum cost paths,” *IEEE Transactions on Systems Science and Cybernetics*, vol. 4, no. 2, pp. 100–107, 1968.
- [12] Y. Chang, L. Ballotta, and L. Carlone, “D-lite: Navigation-oriented compression of 3D Scene Graphs for multi-robot collaboration,” *IEEE Robotics and Automation Letters*, vol. 8, no. 11, pp. 7527–7534, Nov 2023.
- [13] A. Ray, C. Bradley, L. Carlone, and N. Roy, “Task and motion planning in hierarchical 3D Scene Graphs,” 2024, arXiv:2403.08094.
- [14] A. Kurenkov, R. Mart’ in-Mart’ in, J. Ichnowski, K. Goldberg, and S. Savarese, “Semantic and geometric modeling with neural message passing in 3d scene graphs for hierarchical mechanical search,” *2021 IEEE International Conference on Robotics and Automation (ICRA)*, pp. 11 227–11 233, May 31 - June 04 2020.
- [15] R. Talak, S. Hu, L. Peng, and L. Carlone, “Neural trees for learning on graphs,” in *Conference on Neural Information Processing Systems (NeurIPS)*, Dec 06-14 2021.
- [16] A. Rosinol, A. Violette, M. Abate, N. Hughes, Y. Chang, J. Shi, A. Gupta, and L. Carlone, “Kimera: from SLAM to spatial perception with 3D dynamic Scene Graphs,” *Intl. J. of Robotics Research*, vol. 40, no. 12-14, pp. 1510–1546, 2021.
- [17] T. N. Kipf and M. Welling, “Semi-supervised classification with graph convolutional networks,” in *International Conference on Learning Representations (ICLR)*, Toulon, France, April 24-26 2017.
- [18] D. P. Kingma and J. Ba, “Adam: A method for stochastic optimization,” in *International Conference on Learning Representations (ICLR)*, San Diego, CA, USA, May 07 - 09 2015.